



ORIGINAL ARTICLE

Chloride transport modeling for normal and fly-ash concrete using naturally logarithmic apparent diffusion coefficient with considering eutrophication potential effect

Aruz Petcherdchoo^{a,*}, Rafat Siddique^b, Tanakorn Phoo-ngernkham^c

^aDepartment of Civil Engineering, Faculty of Engineering, King Mongkut's University of Technology North Bangkok
 Bangkok, 10800, Thailand

^bDepartment of Civil Engineering, Thapar Institute of Engineering and Technology, Patiala, 147004, India

^cSustainable Construction Material Technology Research Unit, Department of Civil Engineering, Faculty of Engineering and
 Technology, Rajamangala University of Technology Isan, Nakhon Ratchasima, 30000, Thailand

^{*}Corresponding Author: Aruz Petcherdchoo. Email: aruz.p@eng.kmutnb.ac.th

Abstract: This study indicates two issues of available time-dependent diffusion coefficient function; non-smoothness of diffusion coefficient decay, and inconsistency of stable time of diffusion coefficient. A naturally logarithmic apparent diffusion coefficient function is thus developed for closed-form solutions of chloride transport model. The developed model is validated with experimental data, and its generality is ensured by comparing with the finite difference approach. From the study, the stable time of the developed diffusion coefficient appears 2.87-3.21 years after exposure, and the stable time of surface chloride appears 5 years after exposure. Such early appearance of these stable times behaves different from other studies, causing different long-term chloride prediction and concrete service life. Using the developed model, the influence of cover depth and percent fly-ash is determined in service life prediction. Additionally, this study develops a model to predict environmental impact in terms of eutrophication potential, currently considered as an emerging global issue. The developed eutrophication potential model shows that the increase of fly-ash replacement of 0% to 50% reduces such eutrophication potential due to concrete production by as much as 38%. Moreover, the relationships between the service life and the eutrophication potential for normal and fly-ash concrete tend to be linear.

Keywords: Naturally logarithmic apparent diffusion coefficient, stable time, service life, fly-ash concrete, eutrophication potential

1 Introduction

Fly ash, known as a waste by-product in coal power plant, has been utilized to replace cement in concrete structures instead of putting in landfills due to excessive amount of fly ash in countries [1, 2]. Such fly-ash utilization sustainably helps reduce the production of cement which causes a large number of pollutions, such as carbon dioxide, phosphate, and etc. These pollutions detrimentally cause climate change which has been mentioned worldwide. Hence, studies were done to understand features of fly ash and apply it to a wide variety of studies, e.g., fly-ash geopolymer [3, 4], fly-ash usage as fine aggregates replacement [5], and etc. [6].



Chloride attack is one of the detrimental phenomena on reinforced concrete. Thus, studies have been carried out on such topic, e.g., chloride transport in rubber concrete [7], seawater sea-sand usage in flexural concrete members [8], and etc. Another important aspect is about prediction of chloride diffusivity in concrete. Quantitatively, there are two basic approaches; (1) the Fick based empirical formula, and (2) the Nernst-Planck multi-species formulation. Researchers [9, 10] relied on the first one to assess concrete under chemically aggressive environments due to reasons, e.g., fewer input data and simplicity. These make it suitable for probabilistic study [11-13].

In applying the Fick based equation to assess the diffusion of chlorides within concrete, the one-dimensional partial differential equation is expressed as

$$\frac{\partial C}{\partial t} = \frac{\partial}{\partial x} D \frac{\partial C}{\partial x} \quad (1)$$

where C is denoted as the chloride content in terms of position x and time t , and D is denoted as the diffusion coefficient of concrete. To predict the chloride transport within concrete, Crank [14] presented closed-form solutions which mainly depended on the boundary condition on concrete in terms of surface chloride C_s . In these solutions, the material property of concrete was also required in terms of diffusion coefficient D . Both C_s and D can be computed by curve fitting with test data [15].

Focusing on the diffusion coefficient D , studies rely on the idea in Life-365 [15]. Precisely, the diffusion coefficient is expressed to be a time-dependent decay function, and suddenly assumed to be stable after 25-year exposure due to saturation of cement hydration. For this, there are however two issues to be addressed. First, the sudden setting of stable diffusion coefficient at year 25 is inappropriate due to non-smoothness of the diffusion coefficient decay. Specifically, the diffusion coefficient should smoothly approach to a constant due to smooth saturation of cement hydration. Second, Zhang et al. [16] conducted a set of experiments and found that the stable time of apparent and instantaneous chloride diffusion coefficients tended to occur between 1.12 years (410 days) and 9.75 years (3560 days) after exposure, depending water-to-binder ratio (W/B), admixtures and circumstances. So, the sudden setting of stable diffusion coefficient at 25-year concrete age is inconsistent with real practice. To bridge the gap for these two issues, this study develops a new time-dependent diffusion coefficient function embedded in the closed-form chloride transport model for concrete having W/B of 0.45-0.65 as well as percent fly-ash replacement of 0%-50%, and further applies for concrete service life prediction.

Climate change has been concerned worldwide [17-19]. Concrete production for construction was found to be one of the predominant reasons [2, 20], so studies have been done for sustainable concrete production. As such, this study determines the environmental impacts from concrete production, along with developing the chloride transport model for service life prediction of normal and fly-ash concrete. For this topic, there have been studies which determined the service life of chloride-exposed structural concrete having varied compositions including environmental impacts, e.g., CO_2 and carbon price owing to concrete repairs [21], optimized life-cycle-based embodied energy for fly-ash concrete [22], and etc. For example, Pradhan et al. [23] used life cycle assessment to consider various types of environmental impacts. However, they restricted the percent replacement by fly ash (%FA) as only 30%. To bridge this gap, this study further proposes to determine different proportions of replacement by fly ash, with considering the environmental impacts in terms of eutrophication potential (EP). Such kind of environmental impacts is considered here, because the United Nations [24] reported that the eutrophication led to significant adverse influences on coastal ecosystems, e.g., degeneration in fishery products, occurrence of red tides and dead zones, etc. So, the United Nation Environment Programme launched an index of coastal eutrophication via Sustainable Development Goal (SDG) 14.1.1a to connect reporting systems with the worldwide eutrophication monitoring program. More importantly, the United Nations also stated that the eutrophication was an emerging global issue.

2 Problems of Available Models

2.1 Available Chloride Transport Models

The pattern of the closed-form solution for chloride transport modeling mathematically depends upon the form of surface chloride [21]. From the practical standpoint, the surface chloride C_s can be

specified as a time-dependent function [25], such as linear, parabolic, etc. Furthermore, different surface chloride functions can be combined depending on chloride environment and concrete materials [26, 27]. For example, Petcherdchoo [28] proposed closed-form solutions for bilinear surface chloride functions to predict the transport of chlorides in terms of the time after exposure t as follows

$$C_S = C_0 + kt \quad ; \quad 0 \leq t < t_{st} \tag{2a}$$

$$C_S = C_0 + kt - k\Delta t_D \quad ; \quad t > t_{st} \tag{2b}$$

where Eq. (2a) presented the increase of surface chloride C_S prior to t_{st} (the start of the stable time of C_S) as shown in **Fig. 1**. Notably, C_0 was the initial surface chloride at exposure, whereas k was the rate of surface chloride increase per exposure time. In addition, Eq. (2b) represented the constant surface chloride after t_{st} as shown in **Fig. 1**. For this, the last term of Eq. (2b), or $-k\Delta t_D$, accounted for compensating the increase of surface chloride in Eq. (2a) as to stabilize C_S after t_{st} . And, Δt_D was equal to $(t - t_{st})$. Hence, the closed-form solution for Eqs. (2a) and (2b) was, respectively, derived as

$$C(x, t) = C_0 \operatorname{erfc} \frac{x}{2\sqrt{D_a t}} + kt \left\{ \left[1 + \frac{x^2}{2D_a t} \right] \operatorname{erfc} \left[\frac{x}{2\sqrt{D_a t}} \right] - \frac{x}{\sqrt{\pi D_a t}} \exp \left[-\frac{x^2}{4D_a t} \right] \right\} \tag{3a}$$

$$C(x, t) = \begin{cases} C_0 \operatorname{erfc} \frac{x}{2\sqrt{D_a t}} + kt \left(\left[1 + \frac{x^2}{2D_a t} \right] \operatorname{erfc} \left[\frac{x}{2\sqrt{D_a t}} \right] - \frac{x}{\sqrt{\pi D_a t}} \exp \left[-\frac{x^2}{4D_a t} \right] \right) \\ -k\Delta t_D \left(\left[1 + \frac{x^2}{2D_a \Delta t_D} \right] \operatorname{erfc} \left[\frac{x}{2\sqrt{D_a \Delta t_D}} \right] - \frac{x}{\sqrt{\pi D_a \Delta t_D}} \exp \left[-\frac{x^2}{4D_a \Delta t_D} \right] \right) \end{cases} \tag{3b}$$

in which $\operatorname{erfc}[\]$ was the complementary error function. Moreover, x was the distance from exposed surface. In using these two equations, this study proposes to apply Eq. (3a) to determine the value of C_0 , k , and D_a by regression analysis using a set of experimental data. This is shown in Section 4.2. Moreover, this study also proposes to apply Eq. (3b) to predict the transport of chlorides for comparing with a set of long-term experimental data. This is shown in Section 6.2. For D_a in Eqs. (3a) and (3b), this study further proposes an apparent diffusion coefficient in form of naturally logarithmic function in order to remedy issues. These issues are explained in the next section.

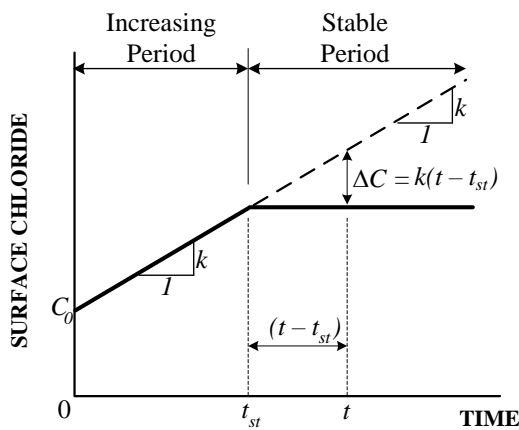


Fig. 1. Bilinearly time-dependent surface chloride [28]

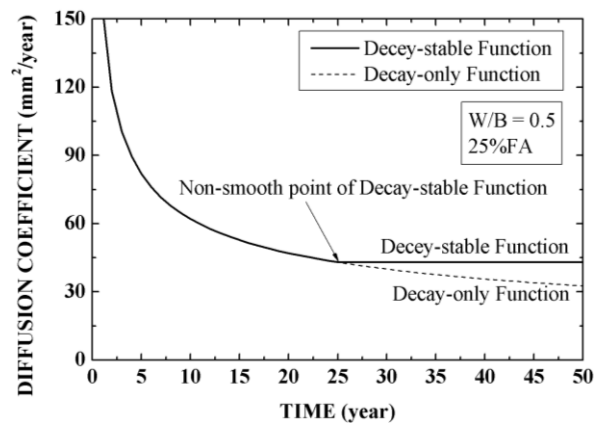


Fig. 2. Diffusion coefficient: decay-stable function (Eq. 7) VS decay-only function (Eq. 4)

2.2 Problems on Available Diffusion Coefficient Functions

According to recent studies, most researches used the time-dependent diffusion coefficient function [15] with respect to the time after exposure t (in year), i.e.,

$$D(t) = D_{\text{ref}} \left(\frac{t_{\text{ref}}}{365t} \right)^m \quad (4)$$

where D_{ref} was the diffusion coefficient at a reference time t_{ref} . If t_{ref} was set as 28 days, Life-365 [15] expressed D_{ref} (m^2/s) as

$$D_{\text{ref}} = D_{28} = 10^{[2.4(W/B)-12.06]} \quad (5)$$

in which W/B was the water-to-binder ratio. Moreover, m in Eq. (4) was the age factor, and equal to $0.2+0.4(\%FA/50)$ in which $\%FA$ was the percent replacement by fly ash. Because $D(t)$ in Eq. (4) is time-dependent, it is inconsistent to directly substitute it into Eqs. (3a) and (3b). This is because Eqs. (3a) and (3b) are derived by assuming D_a as a constant [14]. To remedy the problem, Tang and Gulikers [29] proposed to average $D(t)$ over the time after exposure t as

$$D_a = \frac{\int_{t_{\text{ex}}}^{t+t_{\text{ex}}} D(t)dt}{t} = \frac{D_{\text{ref}}}{1-m} \left[\left(1 + \frac{t_{\text{ex}}}{365t} \right)^m - \left(\frac{t_{\text{ex}}}{365t} \right)^m \right] \left(\frac{t_{\text{ex}}}{365t} \right)^m \quad (6)$$

where t_{ex} was the age of concrete at exposure. For Eq. (6), D_{ref} in Eq. (5) and m were applicable.

Notably, Eq. (4) is a nonlinear decay function with the time after exposure t . However, this is not compatible with real practice, because this decay function will approach to zero in the long run. This is impossible, because concrete will become completely impermeable. But instead, the diffusion coefficient should approach to a constant at a time point. Then, it should become stable in the long run due to saturation of cement hydration. To remedy this problem, Life-365 [15] further recommended to set the decay function to be stable starting at year 25. Thus, Eq. (4) was modified to

$$D(t) = \begin{cases} D_{\text{ref}} \left(\frac{t_{\text{ref}}}{365t} \right)^m ; t \leq 25 \text{ years} \\ D_{\text{ref}} \left(\frac{t_{\text{ref}}}{365 \times 25} \right)^m ; t > 25 \text{ years} \end{cases} \quad (7)$$

In combination with Eq. (5), if the ratio of the water-to-binder (W/B) to the percent replacement by fly ash ($\%FA$) is selected to be 0.5 and 25%, respectively, then $D(t)$ in Eqs. (4) and (7) can be compared as shown in **Fig. 2**. If Eq. (7) which is seen as decay-stable diffusion coefficient is used, there is non-smoothness of $D(t)$ at year 25. This is clearly seen by the sudden deviation from the case of decay-only diffusion coefficient in Eq. (4). Such non-smoothness is inappropriate, because the diffusion coefficient should smoothly approach to a constant due to smooth saturation of cement hydration. This further explains the first issue raised in the Introduction.

For further description [16], the time-dependency of concrete diffusion coefficient depended upon factors, e.g., material properties, water-to-binder ratio, admixtures, etc. For the mechanism, the concrete diffusion coefficient quickly decreased in the early age due to the fast cement hydration. After that, it gradually decreased and became stable, because the cement hydration mechanism was principally saturated.

Considering another form of diffusion coefficient, Riding et al. [30] stated that the diffusivity continued to decay to an ultimate limiting value or D_{ult} . Hence, they further developed Eq. (4) by adding a term to become

$$D(t) = D_{\text{ref}} \left(\frac{t_{\text{ref}}}{365t} \right)^m + D_{\text{ref}} \left(\frac{t_{\text{ref}}}{365t_{\text{ult}}} \right)^m \left(1 - \left[\frac{t_{\text{ref}}}{365t} \right]^m \right) \quad (8)$$

By adding the last term, Riding et al. [30] further stated that the diffusion coefficient after year 25 fell between the case of decay-stable function and the case of decay-only function in **Fig. 2**. However, this additional term cannot solve the second issue stated in the Introduction. In the other word, let us consider Eq. (8). It can be seen that t_{ult} was appropriately selected as 100 years [30], or the ultimate time which the diffusion coefficient approaches to an ultimate diffusion coefficient. However, this selection causes another problem, because t_{ult} is unknown at the beginning. It should be determined after receiving

the diffusion coefficient function from the regression analysis, rather than appropriate selection. For this observation, Riding et al. [30] also stated that it was problematic in selecting t_{ult} . This is related to the second issue as follows.

Considering the study of Zhang et al. [16], the second issue raised in Introduction can be more explained here. In their study, they performed experiments in two marine tidal environmental sites; E1 located in ZhaPu city, China (up to 840-d exposure time), and E2 located in Zhoushan city, China (up to 600-d exposure time). After verifying with exposure tests of eight concrete mixes, they determined the stable time of chloride diffusion coefficients upon considering diffusion coefficient change over time. Considering concrete having W/B of 0.5 and 25%FA as an example, the stable time of the instantaneous chloride diffusion coefficient ranged from 532 days (1.46 years) to 1188 days (3.26 years). These are much different from the assumption of setting the stable time at year 25 in Life-365 [15] as shown in **Fig. 2**.

To alleviate the aforementioned two issues, this study aims to propose an exponential diffusion coefficient and its corresponding apparent diffusion coefficient as explained in the next section.

3 Proposed Diffusion Coefficient

Instead of the decay-stable or the decay-only function as aforementioned, this study proposes an exponential function of time-dependent diffusion coefficient for the smooth decay behavior as

$$D(t) = D_{cst} \left[\frac{1}{1 - \exp(-m_{cst} t)} \right] \quad (9)$$

where D_{cst} is defined as a constant diffusion coefficient which indicates the long-term diffusion coefficient, whereas m_{cst} is an exponential age factor that controls the time-dependent decay in the diffusion coefficient. In order to apply to Eqs. (3a) and (3b), $D(t)$ in Eq. (9) is here averaged over the time after exposure t (year) to obtain a mathematically constant diffusion coefficient, similar to Eq. (6). Hence, it can be expressed as

$$D_a = \frac{\int_{t_{ex}}^{t+t_{ex}} D(t) dt}{t} = \frac{D_{cst}}{m_{cst} t} \left[\ln \left\{ e^{m_{cst}(t+t_{ex})} - 1 \right\} - \ln \left\{ e^{m_{cst}(t_{ex})} - 1 \right\} \right] \quad (10)$$

where D_a is the apparent diffusion coefficient in form of naturally logarithmic function. Similar to Eq. (6), t_{ex} is the age of concrete at exposure. Substituting Eq. (10) into Eqs. (3a) and (3b), the transport of chlorides in normal and fly-ash concrete can be determined from regression analysis and long-term prediction, respectively. This is shown in the following.

4 Applications to Chloride Transport Prediction

The application of the naturally logarithmic diffusion coefficient function of Eq. (10) is here shown by chloride transport modeling for normal and fly-ash concrete. The parameters in Eq. (3a) and (10) are first computed by regression fitting with the experimental data of Chalee et al. [25]. The experiments and the method to compute model parameters are presented as follows.

4.1 Reviewing of Experiments

Experimentally, Chalee et al. [25] used ordinary Portland cement type I and class F fly ash with 30- μ m median particle size from Thailand. In their mix, graded sand and crushed limestone of 19-mm maximum size were utilized. Concrete cube specimens (200 \times 200 \times 200 mm in **Fig. 3**) were cast by replacing cement with fly ash at 0, 15, 25, 35, and 50% by weight of binder, and using W/B at 0.45, 0.55, and 0.65. After 24-hour casting and demolding, the concrete specimens were water-cured 27 days, and sent to a tidal marine environment in Chonburi Province in the Gulf of Thailand, having air temperature between 25 $^{\circ}$ C-35 $^{\circ}$ C. The specimens were daily exposed to wet-dry cycles of seawater with chlorides from 16,000 to 18,000 ppm and sulfate from 2200 to 2600 ppm. At 2-yr, 3-yr, 4-yr, and 5-yr exposures, the specimens were dry-cored with 50-mm diameter. Then, the cored samples were cut at every 10-mm, and each of them was ground to powder. **Fig. 3** shows the example of a test specimen with dry-coring and cutting. To determine the total chloride content, the method specified in ASTM

C1152 [31] were used.

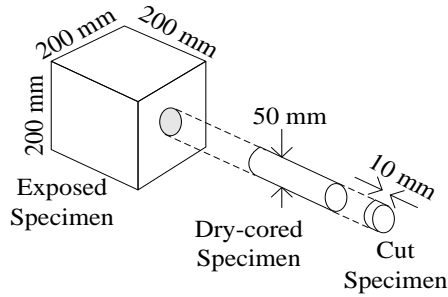


Fig. 3. Test specimen

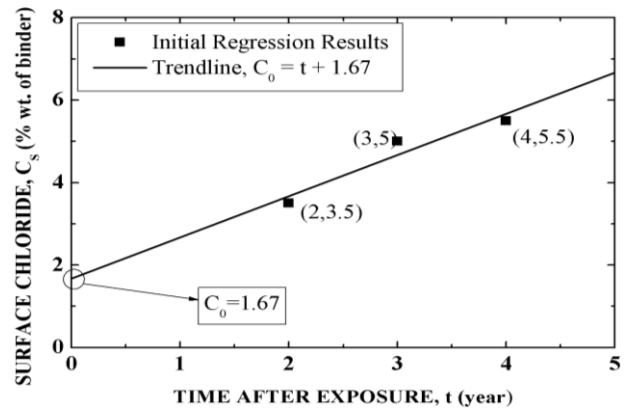


Fig. 4. Evaluation of initial surface chloride, C_0

4.2 Determination of Parameters in Chloride Transport Models

To evaluate all parameters in the chloride transport models, it is first observed from the experiment in Section 4.1. The age of concrete at exposure or t_{ex} is equal to 28 days. Therefore, the naturally logarithmic diffusion coefficient in Eq. (10) is updated as

$$D_a = \frac{D_{cst}}{m_{cst}t} \left[\ln \left\{ e^{m_{cst} \left(t + \frac{28}{365} \right)} - 1 \right\} - \ln \left\{ e^{m_{cst} \left(\frac{28}{365} \right)} - 1 \right\} \right] \tag{11}$$

where the number 365 is used to change the unit into year for unit consistency with the time after exposure t (year). In developing D_a for Eq. (3a), two regression parameters are computed; D_{cst} (mm^2/year) as well as m_{cst} (year^{-1}). For the closed-form solution in Eq. (3a), the corresponding surface chloride in Eq. (2a) is applied. Therefore, there are 2 more regression parameters; C_0 and k . In calculation, the regression analysis is utilized in order to compute all the four regression parameters. In the analysis, the total of the squared differences between the chloride profiles in Chalee et al. [25] and that by the developed model is minimized by varying the regression parameters. Although they exposed the concrete specimens for 2 to 5 years, the regression analysis is here performed at 2- to 4-yr exposure only. After that, this study uses the experimental data at 5-yr exposure for verifying the developed chloride transport models.

Table 1. Examples of C_0 as of the regression analysis

Mix No.	Time after exposure			Average (2- to 4-yr)	Average (0% - 50% FA)
	2-yr	3-yr	4-yr		
I45	1.67	1.67	1.67	1.67	3.2
I45FA15	3.87	3.87	3.87	3.87	
I45FA25	3.48	3.48	3.48	3.48	
I45FA35	3.7	3.7	3.7	3.7	
I45FA50	3.28	3.28	3.28	3.28	

Upon the regression analysis from 2- to 4-yr exposure, the obtained value of k in Eq. (3a) is apparently equal to zero all the cases. For example, let us consider normal concrete having W/B of 0.45. The regression analysis gives C_0 of 3.5, 5, and 5.5% by weight of binder for 2-, 3-, and 4-yr exposure, while k is equal to null for every cases. This appears, because the regression analysis is separately performed in a yearly basis [26]. In order to avoid this, let us consider Fig. 4 which presents the relationship between C_0 and time, including its trendline. The y-intercept of the trendline represents the value of C_0 at the beginning of exposure in Eq. (3a). Specifically, C_0 for the concrete having W/B of 0.45 is set as 1.67% by weight of binder based on using 2-, 3-, and 4-yr exposure data. Table 1 shows the value of C_0 for W/B of 0.45 as an example. By repeating the same process, the values of C_0 for all W/B can be calculated. After that, the regression analysis for all concrete mixes can be performed, and

the value of k , D_{cst} and m_{cst} at 2- to 4-yr exposure is determined as shown in **Tables 2 to 4**.

Table 2. Examples of k as of the regression analysis

Mix No.	Time after exposure			Average (2- to 4-yr)	Average (0% - 50%FA)
	2-yr	3-yr	4-yr		
I45	0.989	1.192	1.026	1.069	0.56
I45FA15	0.507	0.591	0.524	0.541	
I45FA25	0.609	0.586	0.601	0.599	
I45FA35	0.219	0.218	0.218	0.218	
I45FA50	0.390	0.368	0.384	0.381	

Table 3. Examples of D_{cst} as of the regression analysis

Mix No.	Time after exposure			Average (2- to 4-yr)	Average (0% - 50%FA)
	2-yr	3-yr	4-yr		
I45	117.01	116.04	109.04	114.03	2.057
I45FA15	42.03	41.02	36.01	39.69	1.599
I45FA25	41.22	35.14	33.13	36.50	1.562
I45FA35	36.81	29.44	25.94	30.73	1.488
I45FA50	15.12	13.08	14.13	14.11	1.15

Table 4. Examples of m_{cst} as of the regression analysis

Mix No.	Time after exposure			Average (2- to 4-yr)
	2-yr	3-yr	4-yr	
I45	1.609	1.573	1.465	1.549
I45FA15	1.587	1.515	1.502	1.534
I45FA25	1.410	1.579	1.527	1.505
I45FA35	1.352	1.382	1.328	1.354
I45FA50	1.323	1.287	1.178	1.262

As an example, **Fig. 5** compares the chloride contents within concrete from the analysis in Chalee et al. [25] to that in this study for concrete having W/B of 0.45 as well as 0% and 50%FA. Notably, the penetration of chlorides in concrete having 0%FA shown on the left-handed side is more than that with 50%FA shown on the right-handed side, leading to the steeper slope in the case of 50%FA. This is because the increase of fly ash replacement decreases the chloride diffusivity through concrete. This agrees with Chalee et al. [25] who stated that fly-ash concrete was more resistant to chloride penetration than normal concrete, due to more pore size distribution added from fly ash.

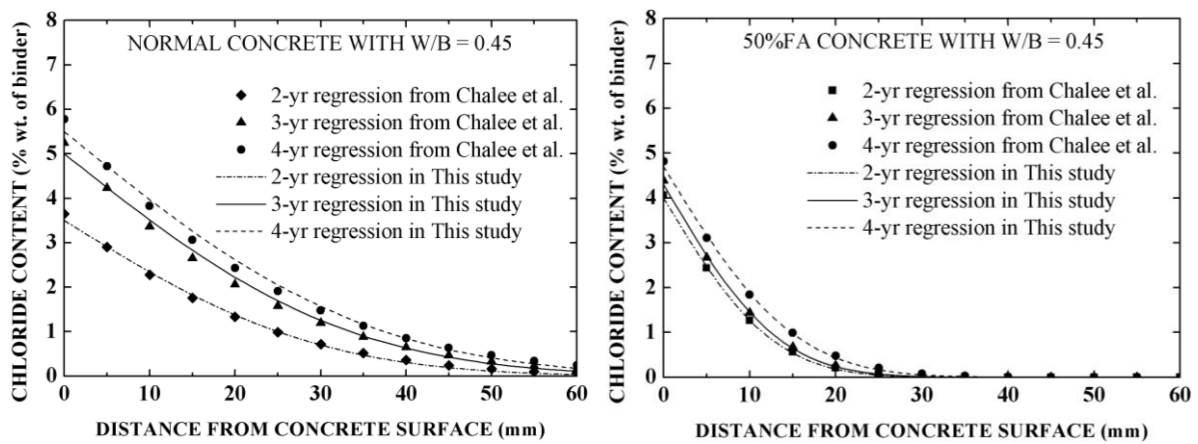


Fig. 5. Chloride profiles from regression analysis up to 4-yr: Chalee et al. [25] VS this study

By further averaging the values of C_0 from 2-yr to 4-yr exposure and over %FA as shown in the last two columns in **Table 1**, the relationship between C_0 and W/B as well as its linear trendline can further be determined as shown in **Fig. 6**. For k , its average values from 2- to 4-yr exposure and 0%FA to 50%FA are shown in **Table 2**. Then, it can be shown that k is averaged over W/B , because it seems independent of W/B . Finally, k is equal to a constant of 0.61 year^{-1} . From the linear equation of C_0 in

Fig. 6 and the constant value of k , the time-dependent surface chloride function can be formulated as $C_s = C_0 + kt = [3.22(W/B) + 1.73] + 0.61t$ (12)

in which C_0 is represented in terms of W/B only, while k is independent of W/B and %FA.

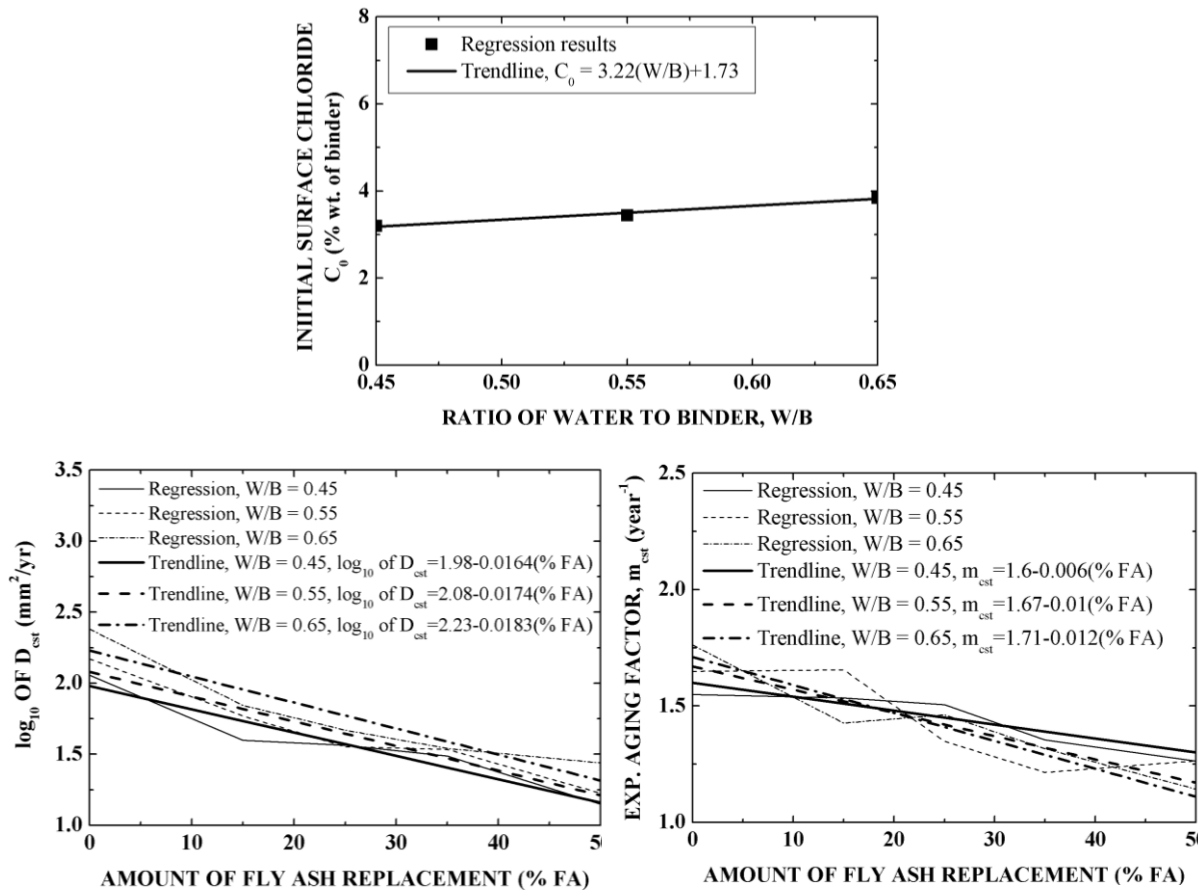


Fig. 6. Evaluation of C_0 , $\log_{10}D_{cst}$, and m_{cst}

By averaging D_{cst} from 2-yr to 4-yr exposure and taking the logarithmic function as shown in **Table 3**, **Fig. 6** represents the relationship between $\log_{10}D_{cst}$ and %FA for W/B of 0.45 to 0.65, and also their trendline including associated three linear equations. From these three linear equations, D_{cst} can further be related to W/B as

$$D_{cst} = 10^{[1.23(W/B)+1.41-\{0.01(W/B)+0.012\}\%FA]} \tag{13}$$

which is represented in terms of both W/B and %FA.

For m_{cst} , the regression analysis results and its average value from 2-yr to 4-yr exposure are shown in **Table 4**. Furthermore, the relationship between m_{cst} and %FA for W/B of 0.45 to 0.65 can be presented in **Fig. 6**. From their trendline as well as three linear equations, m_{cst} can further be determined with respect to W/B as

$$m_{cst} = 0.55(W/B) + 1.36 + \{0.005 - 0.27(W/B)\}\%FA \tag{14}$$

which shows that the decrease rate of the diffusion coefficient relies on both W/B and %FA. The developed models in Eqs. (11) to (14) can further be validated as shown in the next section.

5 Validations of Chloride Transport Models

5.1 Comparison to Experiments

In this section, the apparent diffusion coefficient here developed using the 2-yr to 4-yr experimental

data of Chalee et al [25] is further validated with their 5-yr experimental data. **Fig. 7** compares the chloride contents from the experiments to the chloride profiles predicted using the developed chloride transport models, i.e., Eq. (3a) as well as Eqs. (11) to (14). These show for concrete having W/B of 0.45 and 0.65 and 0%-50%FA. Notably, the predictions agree well with the experiments, although the 5-yr exposure data are not included in the regression computation.

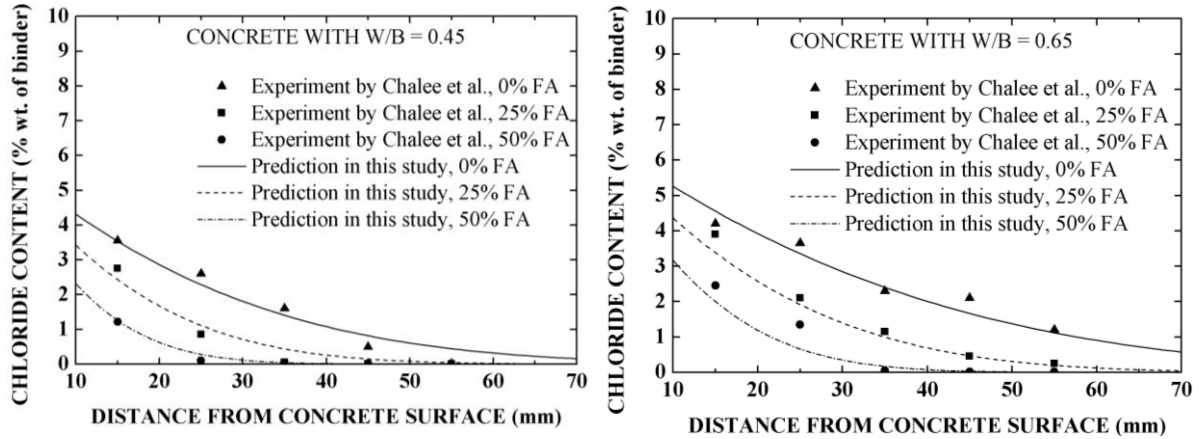


Fig. 7. Chloride profiles at 5-yr exposure: Chalee et al. [25] VS this study

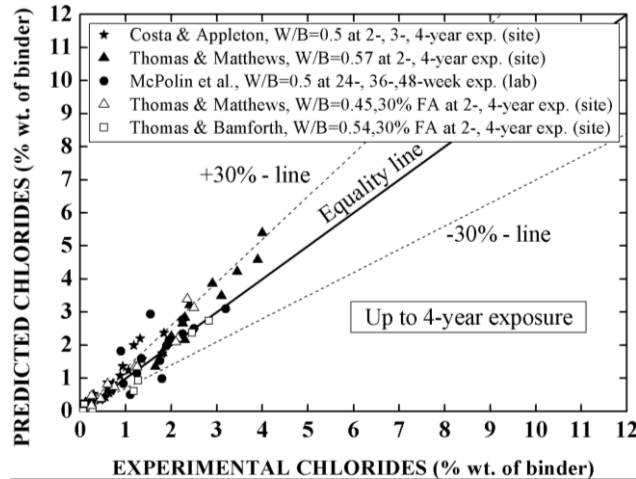


Fig. 8. Predicted VS experimental chloride contents up to 4-year exposure

5.2 Comparison to Other Results

The closed-form solutions embedded with the developed apparent diffusion coefficient can also be validated with other experimental results exposed to chloride environment. **Fig. 8** compares the predicted chloride content, using Eq. (3a) as well as Eqs. (11) - (14), to the experimental chloride content. There are two kinds of concrete materials to be validated; normal and fly-ash concrete. The experimental data for normal concrete are adapted from Costa and Appleton [32] tested at Setubal peninsula facing the Atlantic Ocean, Thomas and Matthews [33] tested in the tidal zone at Shoeburyness, and McPolin et al. [34] tested in simulated chloride environment. Moreover, the experimental data for fly-ash concrete are adapted from Thomas and Matthews [33] tested in the tidal zone at Shoeburyness, and Thomas and Bamforth [35] tested in the splash zone at the England southeast coast. Notably, their W/B and %FA fall within the range used in developing the model this study. The comparisons are shown for 8.5 to 50 mm from concrete surface within 4-yr exposure (the same time period used for the regression analysis in this study). It is found that most of them falls within or near $\pm 30\%$ margin of error. So, the closed-form solution embedded with the apparent diffusion coefficient in form of naturally logarithmic function developed here can well predict the transport of chlorides in normal and fly-ash concrete materials under both natural and simulated chloride environments.

6 Stable Time and Observations

6.1 Exponential Diffusion Coefficient

Section 2.2 mentions that there are two issues in the available time-dependent diffusion coefficient. First, it is inappropriate to assume that the time-dependent diffusion coefficient suddenly becomes a constant at year 25 as shown in Eq. (7) and **Fig. 2** (decay-stable function). But instead, it should smoothly approach to a constant due to smooth saturation of cement hydration. Second, it is evident that the stable time based on the study of Zhang et al. [16] occurs earlier than 25 years as summarized in **Table 5**, in which *E1* and *E2* refer to two marine tidal environments in China.

In order to alleviate such two aforementioned issues, this study therefore proposes a time-dependent diffusion coefficient in terms of an exponential function in Eq. (9). To show its effectiveness, the proposed time-dependent diffusion coefficient is compared to the time-dependent diffusion coefficient developed for the previous study by Petcherdchoo [26]. This is compared, because both studies utilize the same experimental data from Chalee et al. [25] for regression analysis to develop their chloride transport models. In the comparison, this study uses Eqs. (9), (13), and (14), whereas the previous study used Eq. (4) and the following equation

$$D_{ref} = D_{28} = 10^{[1.776+1.364(W/B)] + [5.806 - 18.69(W/B)] [%FA]} \quad (15)$$

which was dependent on both *W/B* and %*FA*.

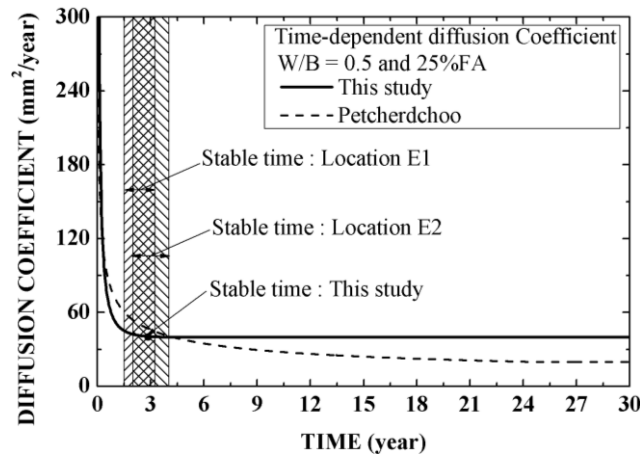


Fig. 9. Stable time of diffusion coefficient in this study VS Petcherdchoo [26]

Fig. 9 shows the example of the comparison for concrete having *W/B* of 0.5 and 25%*FA*. It seems that the early-age diffusion coefficient of this study and Petcherdchoo [26] behaves quite compatible in an average sense, because they are developed using the same experimental data. In addition, the diffusion coefficient in the previous study time-dependently decays, and suddenly becomes stable after 25 years. However, the diffusion coefficient in this study continues to decay time-dependently at the early age. And, it is approximately equal to 40.5 mm²/year at 2.87 years. This is the starting time of the diffusion coefficient to approach to the stable value of D_{cst} (39.8 mm²/year) as calculated by using Eq. (13). In the other word, the change of the time-dependent diffusion coefficient is so low that it is considered stable after 2.87 years. Moreover, the stable time of 2.87 years falls within the range of the stable time for the locations *E1* (1.46 to 3.26 years) and *E2* (1.97 to 4.03 years) in the study of Zhang et al. [16] as shown by two shaded areas in **Fig. 9**. However, the diffusion coefficient from the previous study by Petcherdchoo [26] still continues to decay after 25 years. The difference of the diffusion coefficient between this study and Petcherdchoo [26] causes different long-term prediction for chloride transport through concrete as well as different service life of concrete under chloride attack [16].

Using the same computation, the stable time calculated by Eq. (9) developed in this study for the other mixes can be determined and compared to the stable time for the locations of *E1* and *E2* in the study of Zhang et al. [16] as shown in **Table 5**. It is seen that the stable time estimated from this study mostly falls within that estimated from both *E1* and *E2*. Except normal concrete having *W/B* of 0.6, the

stable time estimated from this study falls outside that estimated from E2 around 7% difference.

Table 5. Stable time of diffusion coefficient

Mix	Stable time (years)		
	Zhang et al. [16]		This study
	<i>E1</i>	<i>E2</i>	
I45	1.33-3.38	2.16-4.46	3.19
I50	1.49-3.83	2.35-3.94	3.21
I50FA25	1.46-3.26	1.97-4.03	2.87
I60	1.8-4.67	3.23-7.37	3.00

6.2 Time-dependent Surface Chloride

In Section 5.2, **Fig. 8** shows the comparison between the predictions in this study using Eq. (3a) as well as Eqs. (11) to (14) and the experimental results. For example, the comparisons with Thomas and Matthews [33] and Thomas and Bamforth [35] up to 4-yr experimental exposure show good trend, as mostly within $\pm 30\%$ margin of error. In addition to 4-yr exposure, they also conducted the experiments during 6- to 10-yr exposure period. For these periods, **Fig. 10a** further shows the comparison between their experimental data and the predictions in this study calculated within 8.5 to 45 mm from concrete surface. Apparently, the comparisons with Thomas and Bamforth [35] tend to fall within or near $\pm 30\%$ margin of error. However, the comparison with Thomas and Matthews [33] obviously falls above $+30\%$ margin of error. Specifically, the model developed in this study predicts higher chloride contents.

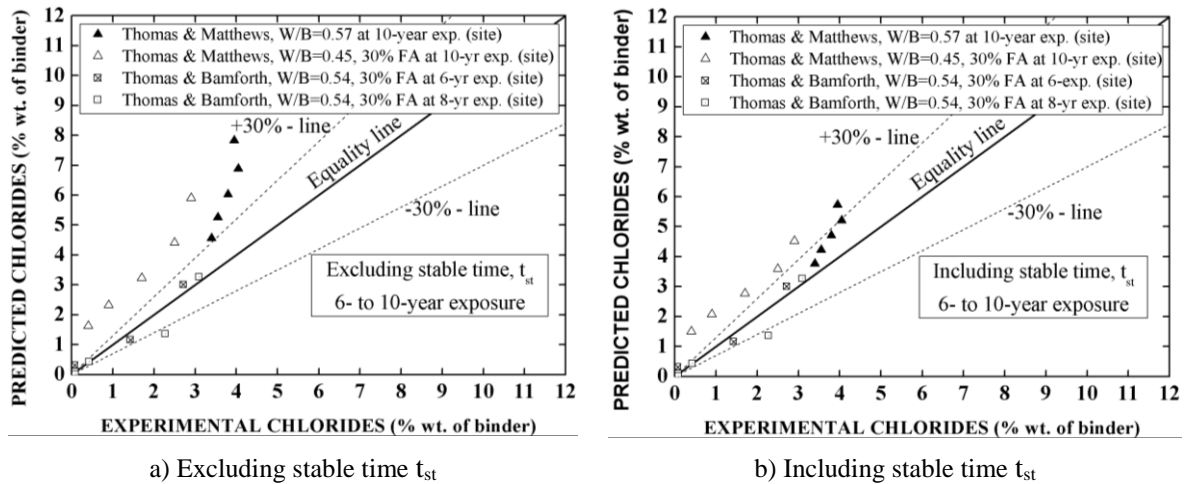


Fig. 10. Predicted VS experimental chloride contents for 6- to 10-year exposure

In attempting to remedy the difference in **Fig. 10a**, there are two factors to be determined; surface chloride and diffusion coefficient. Considering the time-dependent surface chloride, Eq. (2a) is used leading to the closed-form solution in Eq. (3a). For reducing the predicted amount of chlorides in concrete, Eq. (2b) is additionally utilized in combination with Eq. (3b). In the other word, Eq. (2b) is used for the constant surface chloride after the time t_{st} as shown in **Fig. 1**, whereas Eq. (3b) is accordingly used for determining the diffusion of chlorides. In Eq. (3b), Eqs. (11) to (14) are applicable. However, there is still an unknown; the stable time of surface chloride (or t_{st}) in Δt_D , which is equal to $(t-t_{st})$. For this unknown, Life-365 [15] showed the possible time that the surface chloride started to stabilize at 0.8% by weight of concrete after 10-yr exposure for marine splashing zone, and at 0.6% by weight of concrete after 15-yr exposure or more for the atmosphere near coastal area. Moreover, Ehlen et al. [36] presented that the stable time was equal to 7.4 years in the area within New York, USA, for surface chloride buildup to the maximum of 0.8% by weight of concrete. And, it was equal to 3.8 years in the area within Toronto, Canada for the maximum of 1% by weight of concrete. However, the source of chlorides in Toronto expectedly comes from deicing salts. In this study, the stable time t_{st} in Eq. (3b) is simply determined by iterative trial until the difference of chloride contents tends to be about $+30\%$ margin of error. **Fig. 10b** shows the comparisons after using t_{st} of 5 years. Apparently, the comparisons

for normal concrete having W/B of 0.57 is drastically improved, and mostly falls within +30% margin of error. However, the comparison for concrete having W/B of 0.45 and 30%FA falls near +30% margin of error, while showing some reduction. This occurs, because of the effect of the second factor, i.e., diffusion coefficient. For more explanation, the diffusion coefficient for this concrete is considered as follows. Thomas and Matthews [33] calculated the constant diffusion coefficient for this fly-ash concrete as equal to 14.16 mm²/year. At 10-year exposure, D_a using Eqs. (11), (13), and (14) in this study is equal to 34.60 mm²/year, whereas that using Eqs. (5) and (6) in Life-365 [15] is equal to 64.95 mm²/year. In the other word, this study and Life-365 [15] give higher diffusion coefficient than Thomas and Matthews [33] by 2.5 and 4.6 times, respectively. However, all of them fall within the same order. To compensate this difference, further development on the chloride transport models must be carried out. In the other word, a set of long-term experimental data is required to update the chloride transport models, in particular, the diffusion coefficient at 10-year exposure.

Both linear and bilinear surface chloride functions, respectively, in Eq. (2a) and a combination of Eqs. (2a) as well as (2b), used for predicting the chloride contents in **Figs. 10a** and **b**, can also be compared with the parabolic surface chloride function developed in the previous study by Petcherdchoo [26]. For instance, **Fig. 11** compares concrete having W/B of 0.45 and 0.57. Around the beginning, the linear surface chloride is the same as the bilinear one, but higher than the parabolic one. During 2-yr to 4-yr exposure, they tend to be identical, because of using the same experimental data in the regression analysis to develop them. After that, the linear and parabolic surface chloride continue to increase linearly and parabolically, respectively. Expectedly, the bilinear one however starts to stabilize from year 5. The difference of these surface chloride causes different long-term prediction of chloride transport within concrete and different service life of concrete under chloride attack.

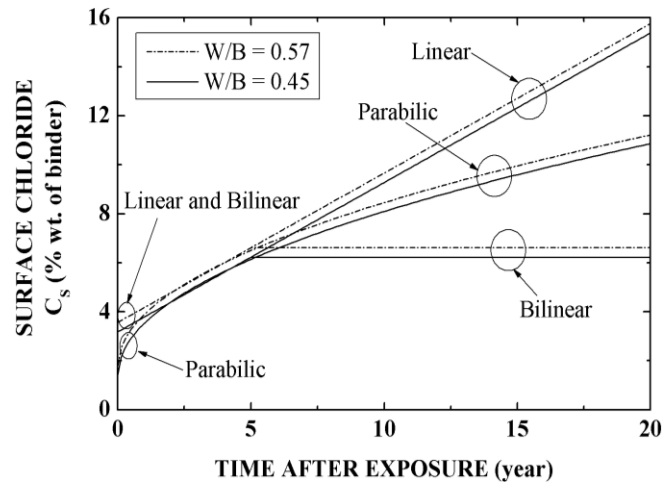


Fig. 11. Linear, bilinear, and parabolic surface chloride functions

7 Further Discussions

7.1 Generality of Developed Diffusion Coefficient Function

The apparent diffusion coefficient in term of naturally logarithmic function D_a embedded in the closed-form solutions for chloride transport modeling by using Eqs. (3a) and (3b) is here proposed by considering mathematical consistency of both C_s and D_a . As explained in Section 4.2, D_a in Eq. (11) is developed and derived by calculating its average value over time. In order to check its generality, this study compares the developed D_a with a numerical computation, such as the finite difference approach (FDA) [26]. Considering the FDA in the comparisons, D in Eq. (1) is substituted with $D(t)$. Hence, the Crank-Nicolson based finite difference can be shown for the time-dependent diffusion coefficient as

$$\frac{c_{i,j+1} - c_{i,j}}{\Delta t} = \frac{1}{2} \left[\frac{D_{j+1} (c_{i+1,j+1} - 2c_{i,j+1} + c_{i-1,j+1})}{(\Delta x)^2} + \frac{D_j (c_{i+1,j} - 2c_{i,j} + c_{i-1,j})}{(\Delta x)^2} \right] \quad (16)$$

in which $c_{i,j}$ is denoted as the chloride content at the mesh point i and time j , respectively, while D_j is the diffusion coefficient at time j . Moreover, Δx and Δt are the size of the mesh point (1 mm) and the incremental time step (1 week), respectively. In utilizing the finite difference formulation in Eq. (16), C_S in Eqs. (2a) and (2b) is used in combination with Eq. (12) and the 5-year stable time t_{st} . Moreover, the exponential diffusion coefficient in Eq. (9) is used in combination with Eqs. (13) and (14). There are two observations for this comparison. First, the surface chloride C_S is bilinear. Second, the exponential diffusion coefficient $D(t)$ is used in the finite difference computation instead of the apparent diffusion coefficient D_a . This is because D_a is used to satisfy the assumption of constant diffusion coefficient in the closed-form solutions in Eqs. (3a) and (3b). However, the finite difference computation does not need to assume the constant diffusion coefficient for solving Eq. (1).

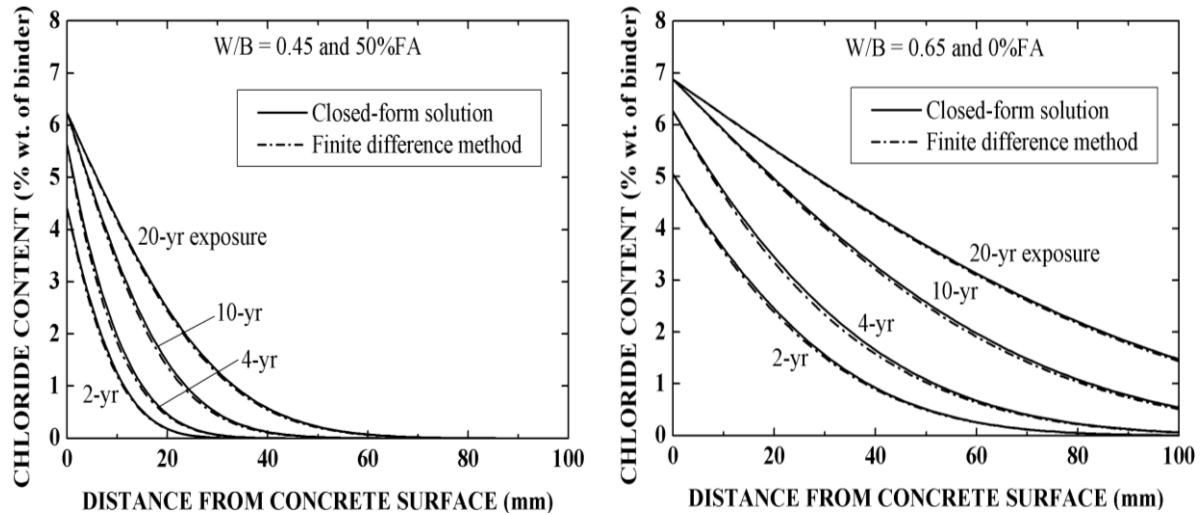


Fig. 12. Generality test of the developed model VS finite difference approach

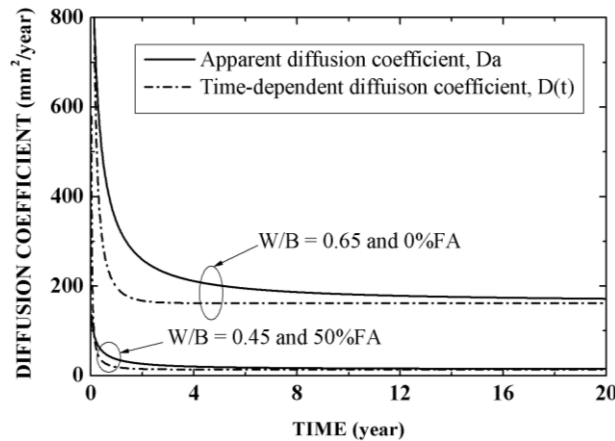


Fig. 13. Comparison between D_a and $D(t)$ developed in this study

In checking the generality, this study evaluates two cases, i.e., (1) concrete having W/B of 0.45 and 50% FA , and (2) normal concrete having W/B of 0.65. Moreover, the evaluation is considered up to 20-yr exposure, because it is expected that there will be at least one intervention on concrete structures after 20 years, such as repair or maintenance. This intervention is expected to change the amount of chlorides in concrete. Fig. 12 compares the predictions by the closed-form solutions and the FDA. There are three main observations. For the first observation, the stable time of the surface chloride is chosen to start from year 5, hence the surface chloride at years 10 is equal to that at year 20. Second, the amount of chlorides in each figure agrees well with each other, although small discrepancy is observed. This discrepancy happens, because D_a in the closed-form solutions is higher than $D(t)$ in the FDA. Such discrepancy also agrees with the discussion in the study of Zhang et al [16]. For more explanation, Fig. 13 shows the difference between D_a and $D(t)$ for two example cases of concrete. The difference occurs,

because D_a in Eq. (11) is derived by averaging $D(t)$ in Eq. (9) over the time after exposure t . Nevertheless, with higher value of D_a , more penetration of chlorides can be expected while leading to more conservative concrete due to higher chloride prediction. For the third observation, **Fig. 13** indicates that when the exposure time approaches to 20-yr exposure, D_a tends to be equal to $D(t)$. This occurs, because the value of $D(t)$ as shown in **Fig. 13** almost becomes a constant and also approaches to the constant value of D_a . As a result, the predictions of chlorides by the closed-form solutions and the FDA tends to give almost the same results at 20-yr exposure as shown in **Fig. 12**.

7.2 Design Service Life

The main purpose of developing the apparent diffusion coefficient here is to assess the service life of structural concrete under chloride environment [37, 38]. Thus, the service life of structural concrete is assessed by considering three cases, i.e., (1) fly-ash concrete having W/B of 0.45 and 50% FA , as well as (2) and (3) normal concrete having W/B of 0.45 and 0.65, respectively. As an example, the amount of chlorides with respect to the depth of concrete having W/B of 0.45 and 50% FA is considered in the previous section in **Fig. 12**. Apparently, the amount of chlorides increases with time.

The key point is to monitor the amount of chlorides at the critical location of reinforcing bar surface, so-called concrete cover depth. According to literatures [39, 40] and the recommendations in the Thai standard, this study selects to monitor at 60 and 80 mm as two representative values. Using Eqs. (3a) and (3b) in combination with Eqs. (11) to (14), the amount of chlorides for concrete at the cover depth of 60 and 80 mm is determined as shown in **Fig. 14**.

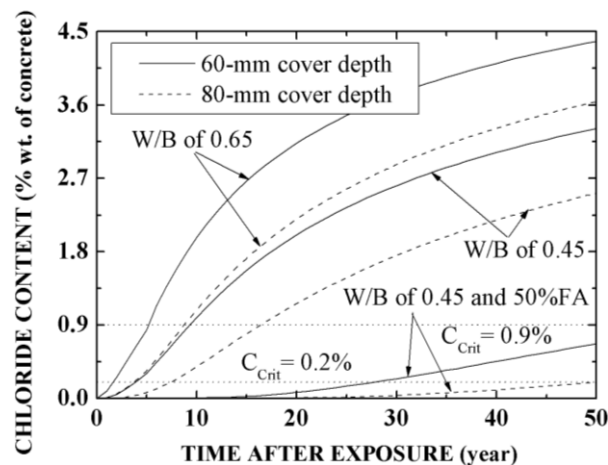


Fig. 14. Prediction of time-dependent chloride content at 60 and 80 mm from concrete surface

Table 6. Service life of three cases for 60- and 80-mm cover depth

Mix No.	Service life (year)	
	60-mm cover depth	80-mm cover depth
I45FA50	28.4	50
I45	9.7	16.8
I65	5.2	9.06

To design structural concrete for a corrosion-free condition, the critical amount of chlorides to initiate the corrosion at the surface of reinforcement was of significance [41]. For this, Angst et al. [42] stated that the critical values reduced with increasing the percent replacement by fly ash. Accordingly, this study applies the critical value from Chalee et al. [25]. In other words, the critical value for initiating rebar corrosion is equal to 0.9% or 0.2% wt. of binder for 0% FA or 50% FA , respectively. Using **Fig. 14**, the corrosion-free service life of three example concretes with the 60-mm and 80-mm cover depth is estimated as shown in **Table 6**. Obviously, by increasing the cover depth from 60 to 80 mm (or 33% increase), the service life increases by 76% (28.4 to 50), 73% (9.7 to 16.8), 74% (5.2 to 9.06) for concrete having W/B of 0.45 and 50% FA , having W/B of 0.45, and having W/B of 0.65, respectively. Moreover, increasing of replacement by fly ash by 50% in concrete having W/B of 0.45 increases the

service life by 193% (9.9 to 28.4) for 60-mm cover depth, and 198% (16.8 to 50) for 80-mm cover depth. Considering the concrete having *W/B* of 0.45 and *W/B* of 0.65, increasing of *W/B* by 44% increases the service life by 87% (5.2 to 9.7) for 60-mm cover depth, and 85% (9.06 to 16.8) for 80-mm cover depth. Specifically, the service life increases with increasing concrete cover depth, due to more distance of chloride transport from concrete surface to reinforcement. In addition, the service life also increases with increasing the percent replacement by fly ash, due to increasing chloride diffusion resistance by more pore size distribution added from fly ash [25]. However, the service life increases with decreasing *W/B*, due to decreasing concrete porosity.

7.3 Comparative Study on Eutrophication Potential (EP)

As mentioned in Section 1, the eutrophication led to significant adverse influences on coastal ecosystems, e.g., the degeneration in fishery products, the occurrence of red tides and dead zones, etc. [24]. Furthermore, a report [43] informed that the eutrophication occurred due to the existence of excessive phosphorus, nitrogen, and various plant nutrients in a mature marine environment. This further led to developing algae and microscopic creatures on such environmental surface. It also prevented the light penetration and oxygen absorption necessary for underwater life, such as fish and other lives.

In order to study the eutrophication potential (*EP*) related to normal and fly-ash concrete, this study proposes a prediction model in form of the compositions of concrete. Here, the source of eutrophication comes from the production of concrete compositions which consequently cause phosphate, resulting in the enrichment of phosphorus for plant nutrients as aforementioned. To determine this, Cheng et al. [44] reported the amount of *EP* in producing a kilogram of raw materials for concrete production. In the other word, the production of cement, fly ash, fine aggregates, coarse aggregates, and water caused the *EP* by 0.211, 0.00105, 0.00249, 0.0374, and 4.99E-05 g PO_4^{-3} eq., respectively. Furthermore, the study of Chalee et al. [25] reported the compositions for production of 1 m³ concrete as shown in **Table 7** for *W/B* of 0.45 as an example. In combining these data [25, 44], the amount of *EP* (g PO_4^{-3} eq.) for producing each raw materials in 1 m³ concrete can be evaluated as shown in **Table 7**.

Table 7. Concrete compositions and EP in producing 1 m³ of concrete

Mix	Concrete compositions (kg)				<i>EP</i> for compositions (g PO_4^{-3} eq)				Total <i>EP</i> (g PO_4^{-3} eq)		
	<i>C</i>	<i>FA</i>	Aggregates		<i>C</i>	<i>FA</i>	Aggregates				
			Fine	Coa.			Fine	Coa.			
I45	478	-	639	1024	215	101	0	1.59	38.3	0.011	141
I45FA15	406	72		1024	215	86	0.08		38.3	0.011	126
I45FA25	359	119		990	215	76	0.12		37.0	0.011	115
I45FA35	311	167		977	215	66	0.18		36.5	0.011	104
I45FA50	239	239		957	215	50	0.25		35.8	0.011	88

Note: *C*, *FA*, *Coa.*, and *W* mean Cement, Fly Ash, Coarse Aggregates, and Water, respectively.

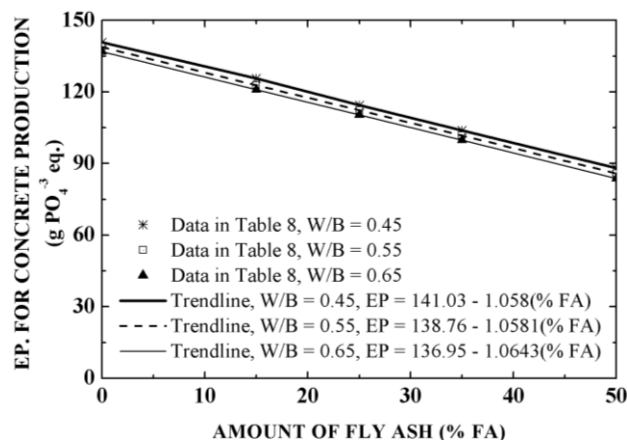


Fig. 15. EP for concrete production and %FA

Using the total amount of *EP* in the last column, **Fig. 15** shows the amount of *EP* versus %*FA*. Incorporating three trendlines for concrete having *W/B* (i.e., 0.45, 0.55, and 0.65), three linear equations can be obtained as shown in the figure. By further determining the coefficients in the three equations, a prediction model for the *EP* (g PO_4^{-3} eq.) in producing 1 m³ of concrete can be formulated as

$$EP = 150.13 - 20.4(W/B) - 1.06(\%FA) \tag{17}$$

where the majority of *EP* comes from the production of cement and coarse aggregates as shown in **Table 7**. Moreover, Eq. (17) also shows that the increase of *W/B* and %*FA* decrease the *EP* due to using less coarse aggregate and cement (see also **Table 7**).

To compare with the service life in Section 7.2, this study considers the *EP* for three cases, i.e., (1) fly-ash concrete having *W/B* of 0.45 and 50%*FA*, as well as (2) and (3) normal concrete having *W/B* of 0.45 and 0.65, respectively. For these, Eq. (17) computationally shows that the increase from 0%*FA* to 50%*FA* reduces the *EP* of concrete having *W/B* of 0.45 by about 38%. Moreover, the increase of *W/B* from 0.45 to 0.65 reduces the *EP* of concrete having %50*FA* by about 4.3%. This reveals that increasing of %*FA* is more efficient in deducting the *EP* than that of *W/B*.

In considering normal and fly-ash concrete, **Fig. 16** relates the service life (SL) to the eutrophication potential. Notably, the all the relationships tend to be linear.

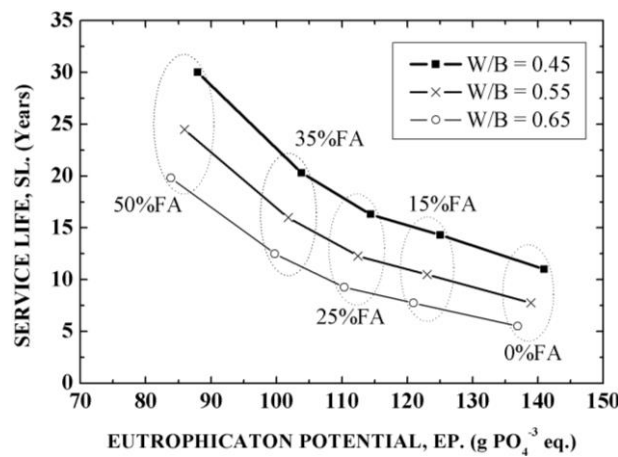


Fig. 16. Service life VS Eutrophication potential

8 Conclusions

This study points out the issues due to the assumptions in the available time-dependent diffusion coefficient. To bridge this gap, this study proposes an exponentially time-dependent diffusion coefficient function and its corresponding apparent diffusion coefficient in form of naturally logarithmic function embedded in the closed-form solutions for chloride transport modeling. According to developing the closed-form solutions, the surface chloride is found in terms of *W/B* only, while the apparent diffusion coefficient is found in terms of both *W/B* and %*FA*. Other than this, the environmental impact model in terms of the eutrophication potential (*EP*) owing to normal and fly-ash concrete production is proposed and studied. From the study, it is found that

1. The apparent diffusion coefficient embedded in the closed-form solutions developed using the experimental data of 2-yr to 4-yr exposure can well predict the transport of chlorides conducted in the same experiment at 5-yr exposure.

2. The chloride contents assessed by the linear closed-form solution embedded with the developed apparent diffusion coefficient function agree well with other experimental results of normal and fly-ash concrete up to 4-yr exposure considering at ±30% margin of error. For 6- to 10-yr exposure data, the bilinear closed-form solution is applied to determine the stable time of surface chloride found as 5 years after exposure.

3. The stable time of the exponential diffusion coefficient function developed here is mostly compatible with that observed in the reference experiment, in spite of around 7% difference found in

some case. Moreover, the stable time estimated in this study falls between 2.87 and 3.21 years depending on W/B and % FA .

4. The generality analysis of the developed apparent diffusion coefficient function by comparing the prediction with the finite difference approach shows well consistency, in spite of small discrepancy. However, such discrepancy leads to more penetration of chlorides, leading to more conservative prediction due to shorter service life.

5. With increasing the cover depth by 33%, the service life increases by 73% to 74%. For 60- or 80-mm cover depth of concrete having W/B of 0.45, the increase of fly ash replacement from 0%-50% increases the service life by 193% or 198%, respectively. For 60- or 80-mm cover depth, the increase of W/B from 0.45 to 0.65 increases the service life by 87% or 85%, respectively.

6. The developed eutrophication potential (EP) model predicts that the increase from 0% FA to 50% FA deducts the EP due to concrete production up to 38%. And, the increase of % FA is more efficient in deducting the EP than that of W/B . Moreover, the relationships between the service life (SL) and the eutrophication potential in producing normal and fly-ash concrete tend to be linear.

7. This study focuses on concrete having W/B of 0.45 to 0.65 and 0% FA to 50% FA . For further study, it is recommended to consider concrete having different W/B and other supplementary materials, for instance, silica fume, slag, and etc.

Acknowledgements

This research budget is allocated by National Science, Research and Innovation Fund (NSRF), and King Mongkut's University of Technology North Bangkok (Project no. KMUTNB-FF-67-B-44 and KMUTNB-FF-67-B-45). This research project was also supported by the NSRF via the Program Management Unit for Human Resources & Institutional Development, Research and Innovation [grant number B40G660036].

CRedit authorship contribution statement

Aruz Petcherdchoo: Conceptualization, Investigation, Formal analysis, Writing – original draft, Funding acquisition, Supervision. **Rafat Siddique:** Writing – review & editing. **Tanakorn Phoo-ngernkham:** Writing – review & editing.

Conflicts of Interest

The authors declare that they have no conflicts of interest to report regarding the present study.

References

- [1] Ping KKL, Cheah CB, Liew JJ, Siddique R, Tangchirapat W, Johari MABM. Coal bottom ash as constituent binder and aggregate replacement in cementitious and geopolymer composites: A review. *Journal of Building Engineering* 2022; 52: 104369. <https://doi.org/10.1016/j.jobe.2022.104369>.
- [2] Petcherdchoo A. Environmental impacts of combined repairs on marine concrete structures. *Journal of Advanced Concrete Technology* 2015; 13: 205-213. <https://doi.org/10.3151/jact.13.205>.
- [3] Uddin Ahmed Shaikh F, Haque S, Sanjayan J. Behavior of fly ash geopolymer as fire resistant coating for timber. *Journal of Sustainable Cement-Based Materials* 2019; 8(5): 259–274. <https://doi.org/10.1080/21650373.2018.1537015>.
- [4] Ganeshan M, Venkataraman S. Durability and microstructural studies on fly ash blended self-compacting geopolymer concrete. *European Journal of Environmental and Civil Engineering* 2021; 25(11): 2074-2088. <https://doi.org/10.1080/19648189.2019.1615991>.
- [5] Joumblat R, Elkordi A, Khatib J, Al Basiouni Al Masri Z, Absi J. Characterisation of asphalt concrete mixes with municipal solid waste incineration fly ash used as fine aggregates substitution. *International Journal of Pavement Engineering* 2023; 24(2): 2099855. <https://doi.org/10.1080/10298436.2022.2099855>.
- [6] Wei Y, Chai J, Qin Y, Xu Z. Compressive behavior and microstructural analysis of low and high volume fly ash concrete containing recycled concrete aggregate. *European Journal of Environmental and Civil Engineering* 2022; 26(12): 6115–6132. <https://doi.org/10.1080/19648189.2021.1934551>.
- [7] Han Q, Yang Y, Zhang J, Dong B. Electrochemical characterization of chloride ion transport in rubber concrete. *Journal of Building Engineering* 2023; 73: 106658. <https://doi.org/10.1016/j.jobe.2023.106658>.

- [8] Li H, Feng Z, Sayed U, Adjei P, Xue X, Wang Z, Corbi O. Flexural performance of bamboo fiber-reinforced concrete mixed with seawater and sea sand. *Structural Concrete* 2024; 25(5): 3731–3748. <https://doi.org/10.1002/suco.202300336>.
- [9] Zhang J, Jin T, He Y, Yu W, Gao Y, Zhang Y. Time dependent correlation of permeability of fly ash concrete under natural tidal environment. *European Journal of Environmental and Civil Engineering* 2022; 26(16): 8477-8501. <https://doi.org/10.1080/19648189.2022.2028191>.
- [10] Yuan W-B, Mao L, Li L-Y. A two-step approach for calculating chloride diffusion coefficient in concrete with both natural and recycled concrete aggregates. *Science of the Total Environment* 2023; 856: 159197. <https://doi.org/10.1016/j.scitotenv.2022.159197>.
- [11] Deby F, Carcassès M, Sellier A. Probabilistic approach for durability design of reinforced concrete in marine environment. *Cement and Concrete Research* 2009; 39: 466-471. <https://doi.org/10.1016/j.cemconres.2009.03.003>.
- [12] Zhang J, Wu H, Du S, Li X, Zhang Y, Wu L. Similarity analysis of randomness in instantaneous chloride diffusion coefficient of concrete under different environmental exposures. *Case Studies in Construction Materials* 2024; 21: e03430. <https://doi.org/10.1016/j.cscm.2024.e03430>.
- [13] Petcherdchoo A. Probabilistic model for single and multiple action costs in maintaining both condition and safety of deteriorating reinforced concrete bridges. *Case Studies in Construction Materials* 2023; 19: e02613. <https://doi.org/10.1016/j.cscm.2023.e02613>.
- [14] Crank J, *The mathematics of diffusion*, Oxford University, 1975.
- [15] Ehlen MA, *Life-365 v2.2.3 program manual*, Life365 Consortium III, 2020.
- [16] Zhang J, Zhou X, Zhang Y, Wang M, Zhang Y. Stable process of concrete chloride diffusivity and corresponding influencing factors analysis. *Construction and Building Materials* 2020; 261: 119994. <https://doi.org/10.1016/j.conbuildmat.2020.119994>.
- [17] Garavaglia E, Tedeschi C. Analysis of the mass and deformation variation rates over time and their influence on long-term durability for specimens of porous material. *Sustainable Structures* 2022; 2(1): 000014. <https://doi.org/10.54113/j.sust.2022.000014>.
- [18] Gu C, Gu H, Gong M, Blackadar J, Zahabi N. Comparison of using two LCA software programs to assess the environmental impacts of two institutional buildings. *Sustainable Structures* 2024; 4(1): 000034. <https://doi.org/10.54113/j.sust.2024.000034>.
- [19] Xia B, Xiao J, Ding T, Guan X, Chen J. Life cycle assessment of carbon emissions for bridge renewal decision and its application for Maogang Bridge in Shanghai. *Journal of Cleaner Production* 2024; 448: 141724. <https://doi.org/10.1016/j.jclepro.2024.141724>.
- [20] Xu P, Zhu J, Li H, Xiong Z, Xu X. Coupling analysis between cost and carbon emission of bamboo building materials: A perspective of supply chain. *Energy and Buildings* 2023; 280: 112718. <https://doi.org/10.1016/j.enbuild.2022.112718>.
- [21] Petcherdchoo A. Repairs by fly ash concrete to extend service life of chloride-exposed concrete structures considering environmental impacts. *Construction and Building Materials* 2015; 98: 799–809. <https://doi.org/10.1016/j.conbuildmat.2015.08.120>.
- [22] Kurda R, Silvestre JD, de Brito J, Ahmed H. Optimizing recycled concrete containing high volume of fly ash in terms of the embodied energy and chloride ion resistance. *Journal of Cleaner Production* 2018; 194: 735e750. <https://doi.org/10.1016/j.jclepro.2018.05.177>.
- [23] Pradhan S, Chang Boon Poh A, Qian S. Impact of service life and system boundaries on life cycle assessment of sustainable concrete mixes. *Journal of Cleaner Production* 2022; 342: 130847. <https://doi.org/10.1016/j.jclepro.2022.130847>.
- [24] United Nations Environment Programme, *Global Eutrophication Watch: a cost-effective interactive assessment of coastal eutrophication on the cloud*. <https://www.unep.org/nowpap/news-and-stories/story/global-eutrophication-watch-cost-effective-interactive-assessment-coastal>, 2024(accessed April 26, 2024).
- [25] Chalee W, Jaturapitakkul C, Chindaprasirt P. Predicting the chloride penetration of fly ash concrete in seawater. *Marine Structures* 2009; 22: 341–353. <https://doi.org/10.1016/j.marstruc.2008.12.001>.
- [26] Petcherdchoo A. Time dependent models of apparent diffusion coefficient and surface chloride for chloride transport in fly ash concrete. *Construction and Building Materials* 2013; 38: 497-507. <https://doi.org/10.1016/j.conbuildmat.2012.08.041>.
- [27] Petcherdchoo A. Service life and environmental impact due to repairs by metakaolin concrete after chloride attack. *Rilem Bookseries* 2015; 10: 35-41. https://doi.org/10.1007/978-94-017-9939-3_5.
- [28] Petcherdchoo A. Closed-form solutions for bilinear surface chloride functions applied to concrete exposed to deicing salts. *Cement and Concrete Research* 2017; 102: 136–148. <https://doi.org/10.1016/j.cemconres.2017.09.007>.
- [29] Tang L, Gulikers J. On the mathematics of time-dependent apparent chloride diffusion coefficient in concrete. *Cement and Concrete Research* 2007; 37: 589–95. <https://doi.org/10.1016/j.cemconres.2007.01.006>.
- [30] Riding KA, Thomas MDA, Folliard KJ. Apparent diffusivity model for concrete containing supplementary

- cementitious materials. *ACI Materials Journal* 2013; 110: 705-713. <https://doi.org/10.14359/51686338>.
- [31] ASTM, Standard test method for acid-soluble chloride in mortar and concrete, C1152, Annual book of ASTM standards, 1997.
- [32] Costa A, Appleton J. Chloride penetration into concrete in marine environment - Part I: Main parameters affecting chloride penetration. *Materials and Structures* 1999; 32: 252-259. https://doi.org/10.1007/b_f02479594.
- [33] Thomas MDA, Matthews JD. Performance of pfa concrete in a marine environment—10-year results. *Cement and Concrete Composites* 2004; 26: 5–20. [https://doi.org/10.1016/S0958-9465\(02\)00117-8](https://doi.org/10.1016/S0958-9465(02)00117-8).
- [34] McPolin D, Basheer PAM, Long AE, Grattan KTV, Sun T. Obtaining progressive chloride profiles in cementitious materials. *Construction and Building Materials* 2005; 19: 666–673. <https://doi.org/10.1016/j.conbuildmat.2005.02.015>.
- [35] Thomas MDA, Bamforth PB. Modelling chloride diffusion in concrete : Effect of fly ash and slag. *Cement and Concrete Research* 1999; 29: 487–495. [https://doi.org/10.1016/S0008-8846\(98\)00192-6](https://doi.org/10.1016/S0008-8846(98)00192-6).
- [36] Ehlen MK, Thomas MDA, Bentz E, Life-365 Service life prediction model version 2.0, 2009.
- [37] Petcherdchoo A. Reliability-based efficiency considering CO2 emission owing to silane treatment on concrete structures under chloride attack. *Case Studies in Construction Materials* 2024; 20: e03081. <https://doi.org/10.1016/j.cscm.2024.e03081>.
- [38] Nath P, Sarker PK, Biswas WK. Effect of fly ash on the service life, carbon footprint and embodied energy of high strength concrete in the marine environment. *Energy and Buildings* 2018; 158: 1694-1702. <https://doi.org/10.1016/j.enbuild.2017.12.011>.
- [39] Chalee W, Teekavanit M, Kiattikomol K, Siripanichgorn A, Jaturapitakkul C. Effect of W/C ratio on covering depth of fly ash concrete in marine environment. *Construction and Building Materials* 2007; 21: 965-971. <https://doi.org/10.1016/j.conbuildmat.2006.03.002>.
- [40] Petcherdchoo A. Sensitivity of service life extension and CO2 emission due to repairs by silane treatment applied on concrete structures under time-dependent chloride attack. *Advances in Materials Science and Engineering* 2018; 2018: 2793481. <https://doi.org/10.1155/2018/2793481>.
- [41] Feng W, Tarakbay A, Memon SA, Tang W, Cui H. Methods of accelerating chloride-induced corrosion in steel-reinforced concrete: A comparative review. *Construction and Building Materials* 2021; 289: 123165. <https://doi.org/10.1016/j.conbuildmat.2021.123165>.
- [42] Angst U, Elsener B, Larsen CK, Vennesland Ø. Critical chloride content in reinforced concrete – a review. *Cement and Concrete Research* 2009; 39: 1122–1138. <https://doi.org/10.1016/j.cemconres.2009.08.006>.
- [43] The Editors of Encyclopedia Britannica, Eutrophication. <https://www.britannica.com/science/eutrophication>, 2024 (accessed December 15, 2024).
- [44] Cheng L, Jin H, Liu J, Xing F. A comprehensive assessment of green concrete incorporated with municipal solid waste incineration bottom: Experiments and life cycle assessment (LCA). *Construction and Building Materials* 2024; 413: 134822. <https://doi.org/10.1016/j.conbuildmat.2023.134822>.